International Conference on Applied Energy 2019
Aug 12-15, 2019, Västerås, Sweden
Paper ID: 475

OPTIMIZATION OF ZIGZAG PASSAGE OF PCHE FOR MOLTEN SALT/S-CO_2 HEAT EXCHANGER

Qianmei Fu, Yuanyuan Zhang, Jing Ding, Weilong Wang, Jianfeng Lu*

School of Material Science and Engineering/School of Intelligent Systems Engineering, Sun Yat-Sen University, Guangzhou, 510006, China

ABSTRACT

Molten salt and S-CO_2 are important high temperature heat transfer media, but molten salt/ S-CO_2 heat exchanger was seldom reported. In present paper, heat transfer in zigzag printed circuit heat exchanger with molten salt and S-CO_2 is simulated and analyzed. Along flow direction, local heat transfer coefficient of S-CO_2 first decreases with Richardson number decreasing in inlet region, and then increases with turbulent kinetic energy rising in outlet region. Performance of PCHE is mainly determined by pressure drop in molten salt passage and heat transfer resistance in S-CO_2 passage. In order to decrease the pressure drop of molten salt, an optimal structure with "sin" passage is proposed. Results show that molten salt pressure drop significantly decreases in the optimal passage, and overall heat transfer coefficient slightly changes, so comprehensive performance of PCHE is improved.

Keywords: heat exchanger, molten salt, supercritical carbon dioxide, numerical simulation

NONMENCLATURE

h	heat transfer coefficient (Wm^{-2} K^{-1})
K	overall heat transfer coefficient (Wm^{-2} K^{-1})
k	turbulent kinetic energy (m^2s^{-2})
p	pressure (Pa)
q	heat flux (Wm^{-2})
q_m	mass flow rate (gs^{-1})
T	temperature (^oC)
u	velocity (ms^{-1})
Greek symbols	
ρ	density (kgm^{-3})
λ	thermal conductivity ($Wm^{-1}K^{-1}$)
μ	viscosity ($kgm^{-1}s^{-1}$)
ν	kinematic viscosity (m^2s^{-1})
Subscripts	
b	bulk
f	fluid

1. INTRODUCTION

Concentrating solar thermal power (CSP) has attracted great attention due to its high efficiency, low operating cost and good scale-up potential [1]. In order to overcome its characteristics of intermittence, thermal energy storage (TES) should be coupled with CPS. Molten salt is a promising thermal energy storage medium due to its diverse properties [2]. In the past decades, supercritical carbon dioxide (S-CO_2) Brayton cycle emerge as a very promising power conversion cycle that can be integrated with current CSP technology for high-efficiency power production [3].

Printed circuited heat exchanger (PCHE) has been demonstrated as a candidate for intermediate heat exchanger (IHX) [4]. During decades, there have been much research investigating the thermal performances of PCHE with four surface geometries, straight, zigzag, S-shaped and airfoil-fin channels. Kim et al. [5] numerically analyzed associated thermal-hydraulic performance in airfoil fin PCHE. Carlson [6] tested the thermal hydraulic performance of S-CO_2 in PCHEs with straight, zigzag and airfoil fin channels. Yoon et al. [7] comparatively analyzed PCHEs with all types of surface geometries including zigzag channels with different channel angles.

According to above studies, it was found that the zigzag PCHE is more economic and has better thermal performance. Hence, the intermediate heat exchanger (IHX) was then recommended to select zigzag PCHE. This paper mainly focuses on designing a molten salt/S-CO_2 PCHE with zigzag passage, and then associated flow dynamic and heat transfer performance is numerically investigated. In order to further optimize the structure and reduce the pressure drop, a new “sin” passage is designed in this paper. By using optimal flow passages, the pressure drop of molten salt can be decreased with

Selection and peer-review under responsibility of the scientific committee of the 11th Int. Conf. on Applied Energy (ICAE2019).

similar heat transfer coefficient, and comprehensive performance can be improved.

2. NUMERICAL MODEL AND CONDITIONS

2.1 Physical model

The geometric model of zigzag PCHE with semi-circular passages is well accepted and studied, and it can provide good efficiency. The detailed structural parameters of zigzag PCHE are shown in Fig. 1. Refer to the structural dimensions of zigzag PCHE, sin PCHE is obtained from sinusoidal curves, as shown in Fig. 2.

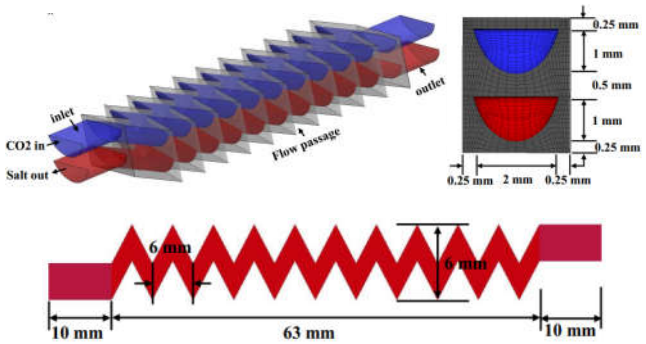

Fig. 1 Structure of zigzag PCHE

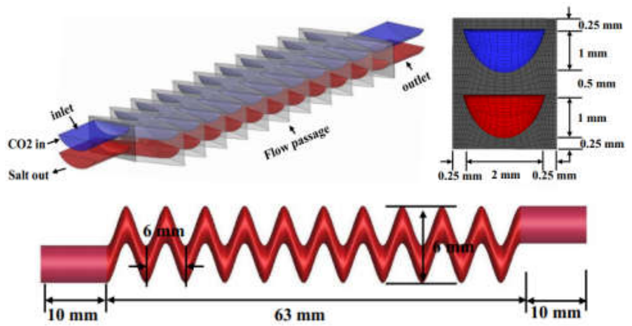

Fig. 2 Structure of sin PCHE

2.2 Calculation conditions

The counterflow heat transfer is used for molten salt and S-CO_2. The thermal physical properties of S-CO_2 can be calculated from NIST Standard Reference Database 23 (REFPROP) Version 9.0 [8]. Mixed nitrate salt is used as heat transfer media [9]. The solid region is made of stainless steel. Periodic conditions are used in the outer boundary of the unit. The outlet pressures of molten salt and S-CO_2 are respectively 0.1 MPa and 20 MPa. For typical case as described as follows, inlet mass flow rate and temperature of S-CO_2 are respectively 0.2 g/s and 35^{o}C, and inlet mass flow rate and temperature of molten salt are set as 0.8 g/s and 400^{o}C.

2.3 Numerical method and validation

The whole flow and heat transfer process is simulated by Fluent 14.5. The computing grid is shown in Fig. 1 and Fig. 2, hexahedral meshes with boundary layer are generated to improve the mesh quality. Three grids with 0.7 million, 1 million and 1.4 million cells are respectively used, and it is found that the relative deviation of temperatures is less than 0.5%, which is acceptable for engineering analysis. Hence, grid with 1.4 million cells is selected as a calculation mesh.

3. RESULTS AND DISCUSSIONS

3.1 Flow and heat transfer of zigzag PCHE

3.1.1 Basic flow dynamic and heat transfer performance

Fig. 3 describes flow and temperature field in middle horizontal sections of molten salt and S-CO_2 flow passages for zigzag PCHE. For counterflow heat transfer, molten salt and S-CO_2 have contrary x-velocities, and the temperature of S-CO_2 heated by high temperature molten salt gradually increases. Along flow direction, x-velocity of S-CO_2 remarkably increases for volume expansion with density dropping, while molten salt velocity changes very little for small density difference. In the case of zigzag PCHE, flow separation occurred after each bending part due to the shape of the edge.

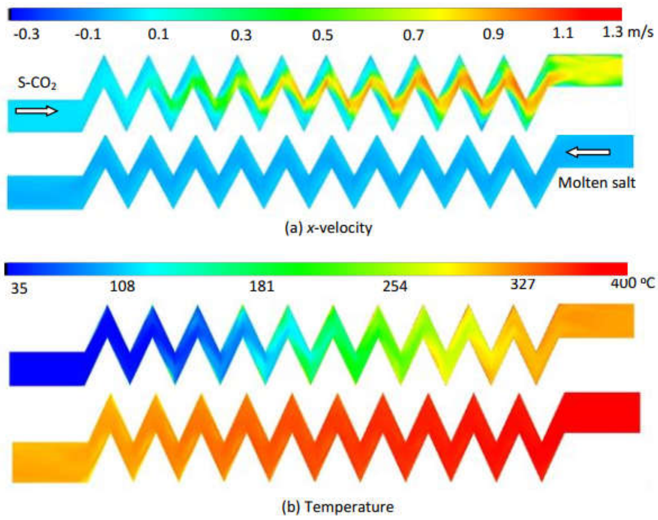

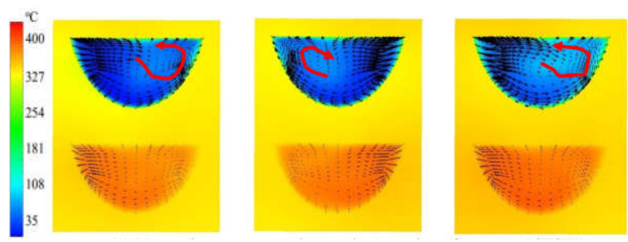

Fig. 4 Vector/temperature in vertical section (Segment Ⅰ/Ⅱ/Ⅲ)

Fig. 4 presents velocity vector/temperature in vertical section in zigzag PCHE. In general, the temperature decreases from main flow of molten salt to solid region and then to main flow of S-CO_2, and the temperature in solid has little difference for high conductivity. In the vertical section of S-CO_2 flow passage (Segment Ⅰ/Ⅱ/Ⅲ), there exist two vortices near the top walls. High temperature S-CO_2 gathers near the top wall by natural convection. Compared with S-CO_2, the velocity of molten salt perpendicular to axis is very little.

3.1.2 Heat transfer for supercritical carbon dioxide

Fig. 5(a) and (b) present pressure and temperature evolution along flow direction in zigzag PCHE. Apparently, the pressure of S-CO_2 periodically drops along flow direction, while that of molten salt linearly decreases. Different from the pressure, bulk temperature of molten salt and S-CO2 gradually changes with no obvious periodicity.

Fig. 5(c) present heat transfer coefficient of molten salt and S-CO2 along flow direction. In inlet region, the vortex caused by buoyancy transports high temperature fluid near the lower wall to the upper region of the passage, and that will benefit the heat transfer. In the middle and outlet regions, the turbulence can be the main factor determining the heat transfer coefficient, and then heat transfer coefficient will increase with turbulent kinetic energy increasing in Fig. 5(d).

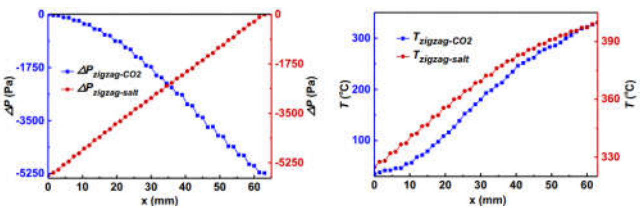

(a)Pressure (b)temperature

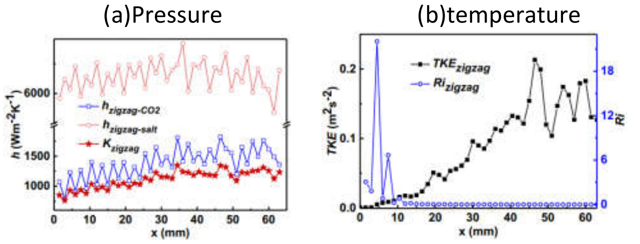

(c)Heat transfer coefficient (d) *Ri* and *TKE*

Fig. 5 Heat transfer of molten salt and S-CO_2 along flow direction

3.2 Heat transfer performance of sin PCHE

3.2.1 Basic flow dynamic and heat transfer performance

Fig. 6 describes flow and temperature field in middle horizontal sections of molten salt and S-CO_2 flow passages for sin PCHE. The velocity vector fields inside the cold channels of sin PCHE was shown in Fig. 7. In the case of the optimum shape, the flow separations were suppressed due to the increased bending angle and the rounded bending edge. This is the main reason for the enhancement of the thermal performance of the optimum design.

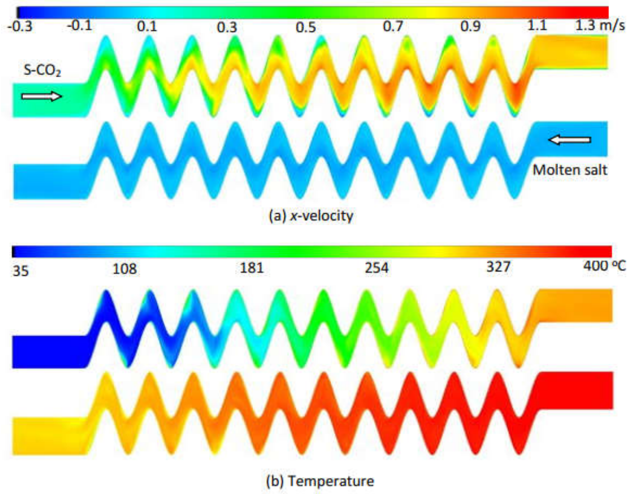

Fig. 6 Flow and temperature field in horizontal section of sin PCHE

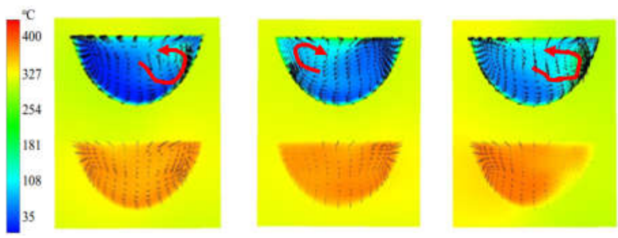

Fig. 7 Vector/temperature in vertical section (SegmentⅠ/Ⅱ/

3.2.2 Heat transfer for supercritical carbon dioxide

Fig. 8(a) and (b) present pressure and temperature evolution along flow direction in zigzag PCHE. Different from the zigzag PCHE, the pressure and bulk temperature of molten salt and S-CO_2 in sin PCHE gradually changes with no obvious periodicity.

Fig. 8(c) present heat transfer coefficient of molten salt and S-CO_2 along flow direction. The trend is similar to zigzag PCHE.

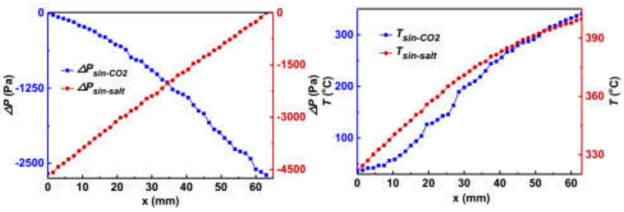

(a)Pressure (b)temperature

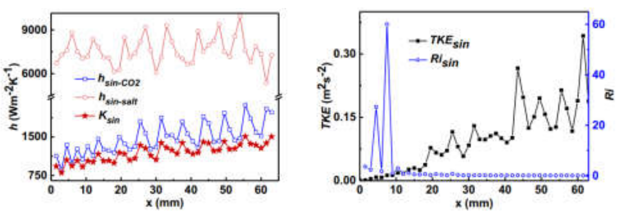

(c)Heat transfer coefficien (d) *Ri* and *TKE*

Fig. 8 Heat transfer of molten salt and S-CO_2 along flow

3.3 Flow and heat transfer with different structure and conditions

Table 1 lists heat transfer performance in zigzag PCHE and sin PCHE with different S-CO_2 flow rate. As S-CO_2 flow rate increases, pressure loss of S-CO_2 quickly increases, and the pressure drop in the sin passage is far less than that in the zigzag passage due to the suppression of the flow separation. With the increase of S-CO_2 flow rate, the total heat transfer coefficient in sin PCHE is higher than zigzag PCHE.

Table 1 Transfer performance with different S-CO_2 flow rate

$G_{m,CO2}$ (g/s)	PCHE	K ($Wm^{-2}K^{-1}$)	h_{CO2} ($Wm^{-2}K^{-1}$)	h_{salt} ($Wm^{-2}K^{-1}$)	P_{CO2} (Pa)	P_{salt} (Pa)
0.1	*Sin*	478	474	10199	890	4508
	Zigzag	482	521	9625	1502	5553
0.2	*Sin*	840	956	9397	2644	4616
	Zigzag	817	944	8553	5228	5700
0.3	*Sin*	1138	1385	9148	4614	4790
	Zigzag	965	1158	8359	7079	5786
0.4	*Sin*	1405	1821	8821	7312	5059
	Zigzag	1112	1371	8164	8930	5871
0.5	*Sin*	1622	2224	5991	10032	5334
	Zigzag	1611	2263	7644	24610	6272
0.6	*Sin*	1821	2635	8327	14926	5582
	Zigzag	2029	2766	12432	31448	6470

4. CONCLUSIONS

In this paper, sin PCHE is first proposed, and the thermal-hydraulic performance of PCHE with zigzag passage and sin passage is further analyzed. Compared with zigzag PCHE, pressure and temperature in sin PCHE has smaller fluctuation. Suppression of the flow separations increases the heat transfer and reduces the pressure drop. The proposed optimization structure can be used as a guide for heat transfer optimization problems that need to compromise between the enhancement of heat transfer and the reduction of pressure drop.

ACKNOWLEDGEMENT

This paper is supported by National Natural Science Foundation of China (U1601215), and Natural Science Foundation of Guangdong Province (2017B030308004).

REFERENCE

[1]Zhang HL, Baeyens J, Degrève J, Cacères G. Concentrated solar power plants: review and design methodology. Renew. Sustain Energy Rev., 2013, 22: 466-481.

[2]Yao Z. Molten salt oxidation: a versatile and promising technology for the destruction of organic-containing wastes. Chemosphere, 2011; 84: 1167-1174.

[3]Ahn Y, Bae S J, Kim M, et al. Review of Supercritical CO2 Power Cycle Technology and Current Status of Research and Development. Nuclear Engineering and Technology, 2015, 47: 647-661.

[4]Li Q, Flamant G, Yuan X, Neveu P, Luo L. Compact heat exchangers: a review and future applications for a new generation of high temperature solar receivers. Renew. Sustain. Energy Rev. 2011, 15: 4855-4875.

[5]Kim DE, Kim MH, Cha JE, Kim SO. Numerical investigation on thermal-hydraulic performance of new printed circuit heat exchanger model. Nucl Eng Des, 2008, 238: 3269-3276

[6]Carlson, MD. "Measurement and Analysis of the Thermal and Hydraulic Performance of Several Printed Circuit Heat Exchanger Channel Geometries," M.S. Thesis, University of Wisconsin-Madison (2012).

[7]Yoon S H, No H C, Kang G B. Assessment of straight, zigzag, S-shape, and airfoil PCHEs for intermediate heat exchangers of HTGRs and SFRs[J]. Nuclear Engineering and Design, 2014, 270:334-343.

[8]http://webbook.nist.gov/chemistry

[9]Lu JF, Shen XY, Ding J, Peng Q. Wen YL. Convective heat transfer of high temperature molten salt in transversely grooved tube. Applied Thermal Engineering, 2013: 61: 157-162.